Supporting Information For:

Luminescent organogels based on triphenylamine functionalized β-diketones and their difluoroboron complexes

Chong Qian, Mingyang Liu, Guanghui Hong, Pengchong Xue, Peng Gong and Ran Lu*

State Key Laboratory of Supramolecular Structure and Materials, College of Chemistry, Jilin University, Changchun 130012, P. R. China

Tel: +86-431-88499179; *E-Mail:* luran@mail.jlu.edu.cn

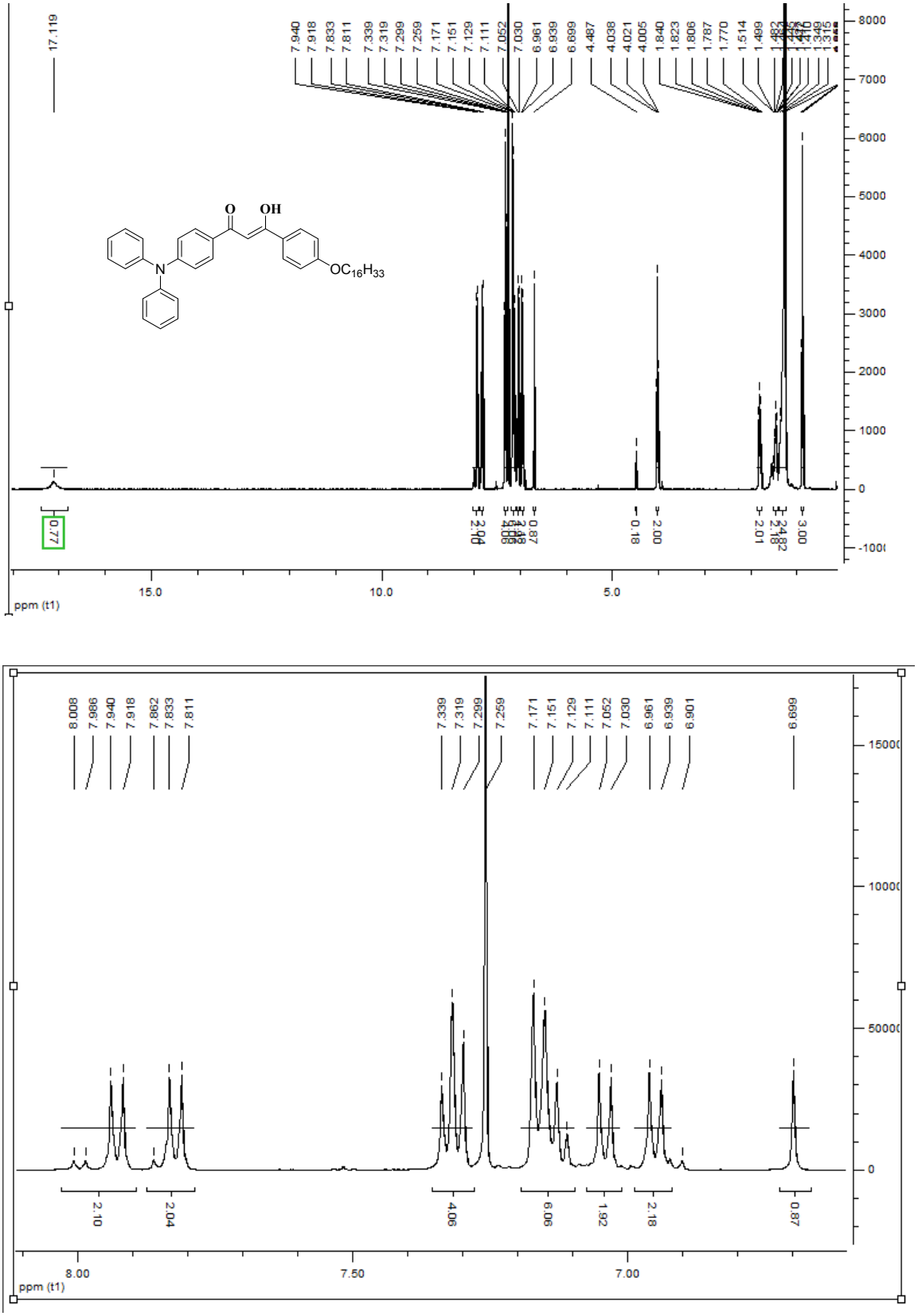

Fig. S1. ^{1}H NMR (400 MHz, $CDCl_3$) spectrum of compound **1**.

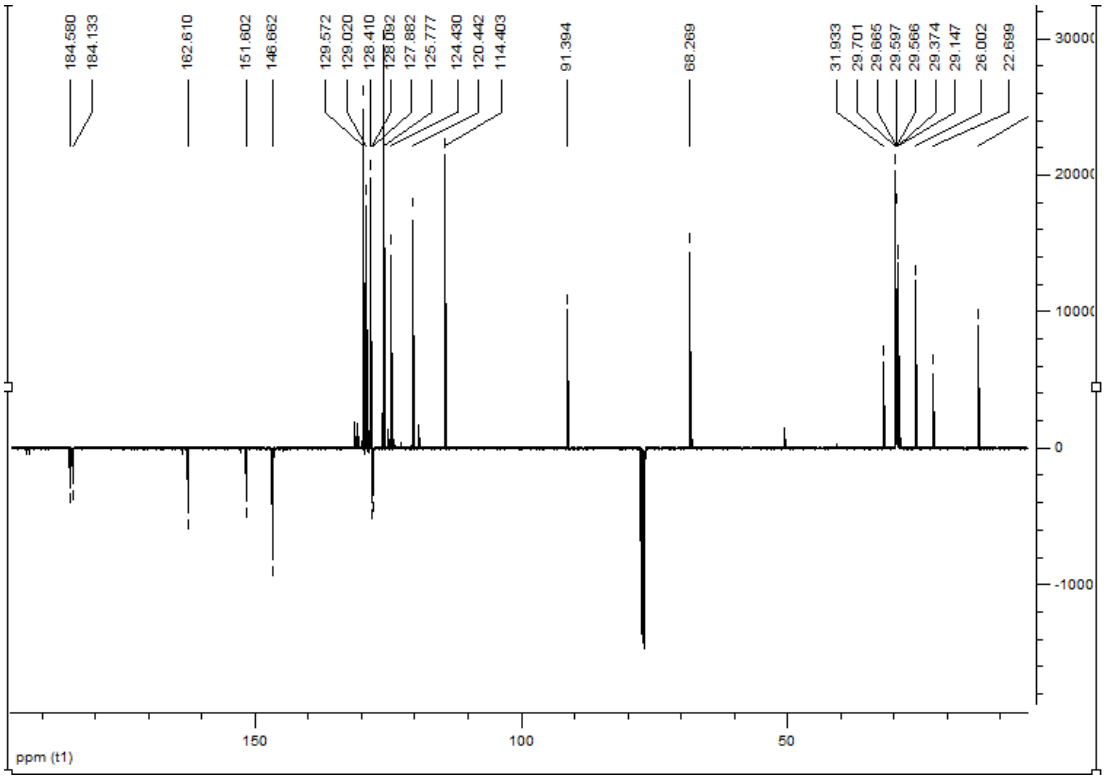

Fig. S2. ^{13}C NMR (125 MHz, $CDCl_3$) spectrum of compound **1**.

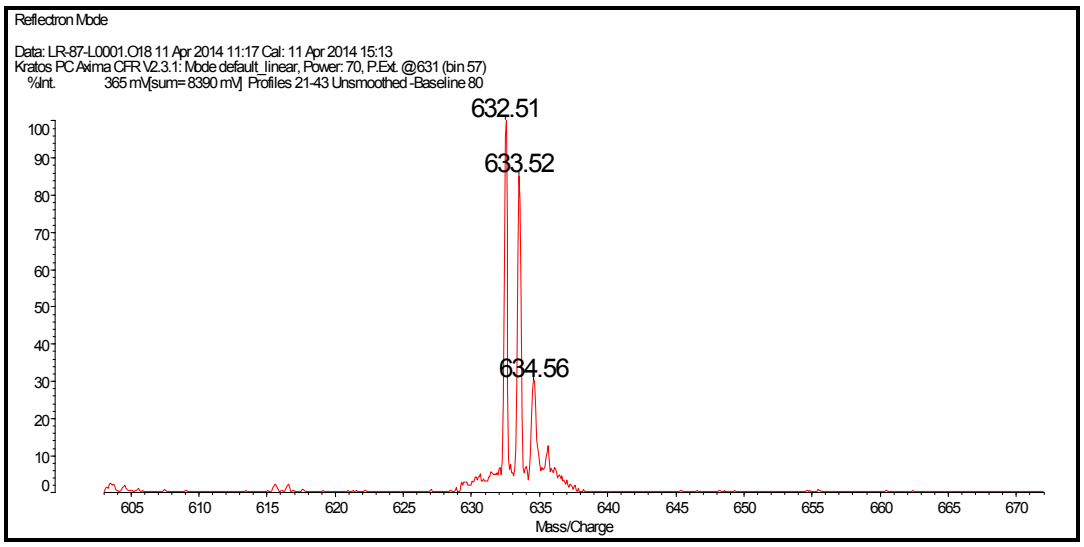

Fig. S3. MALDI/TOF MS spectrum of compound **1**.

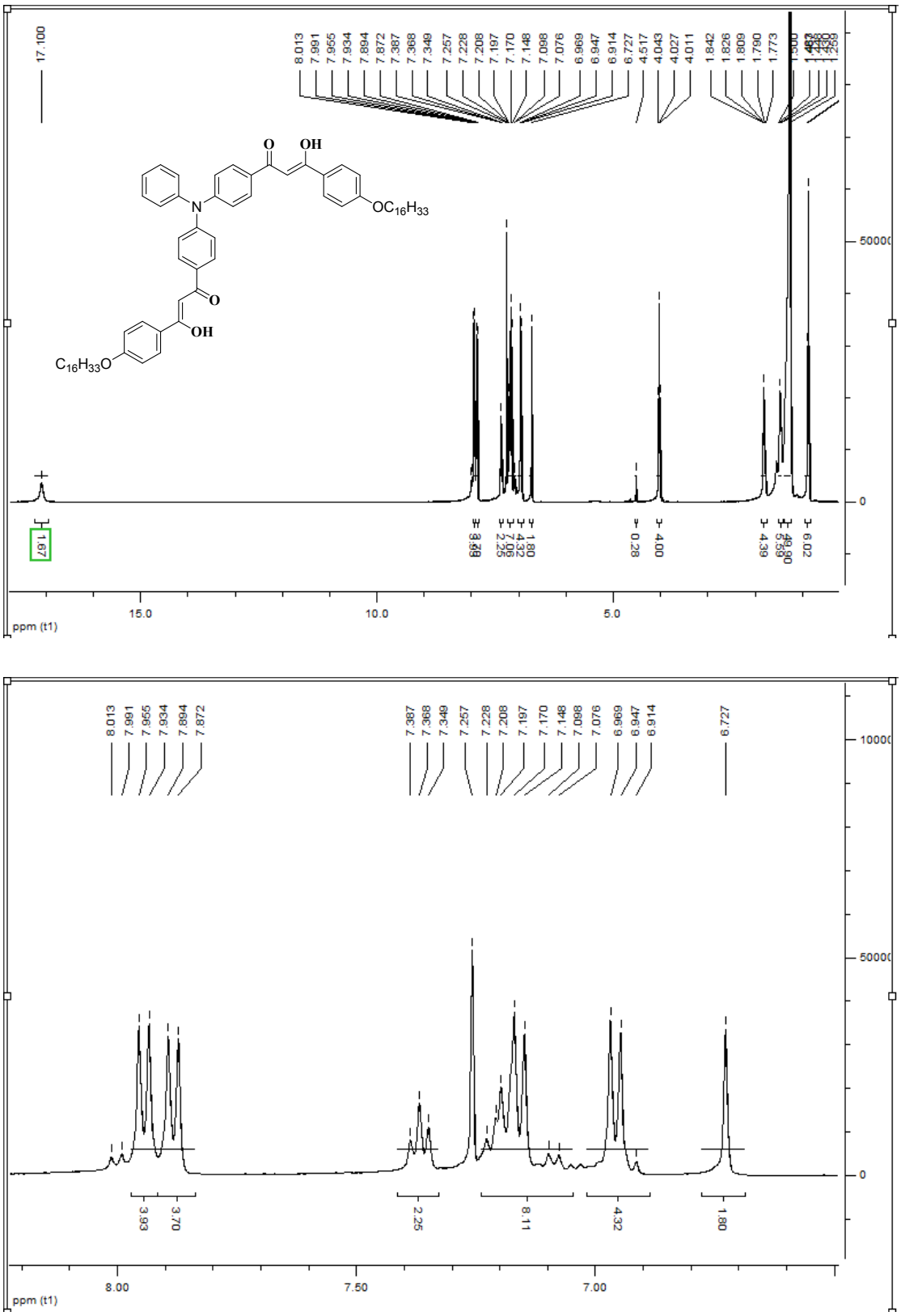

Fig. S4. ^{1}H NMR (400 MHz, $CDCl_3$) spectrum of compound **2**.

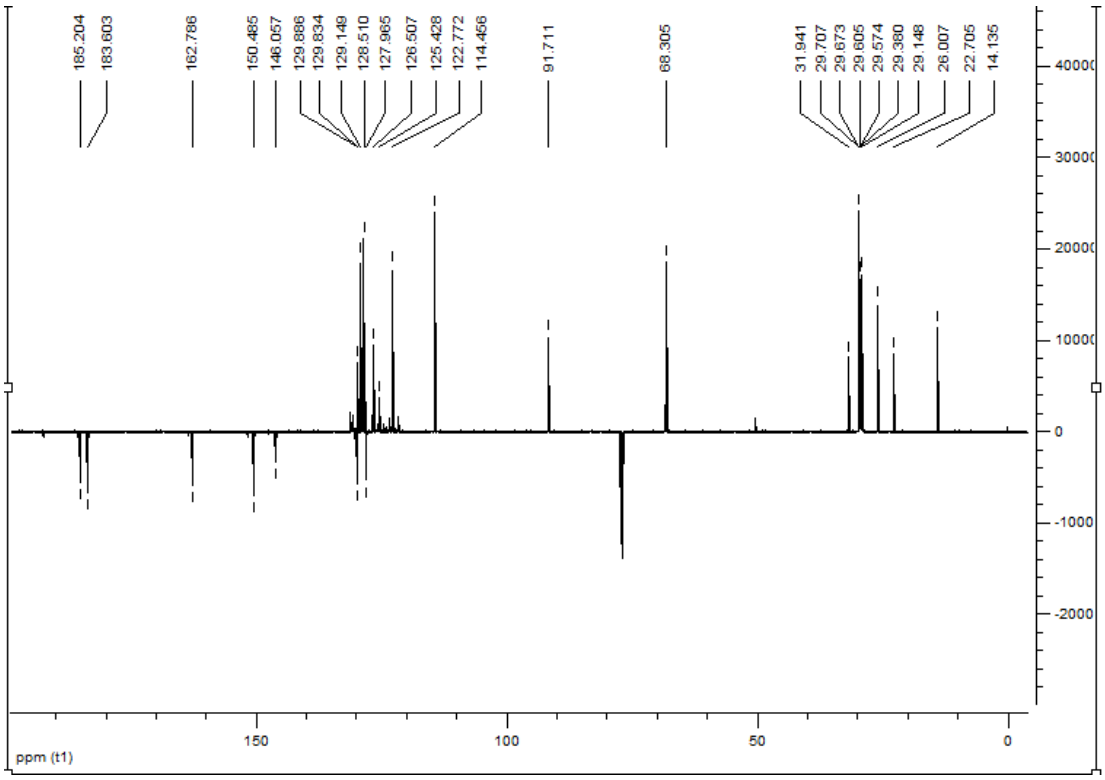

Fig. S5. ^{13}C NMR (125 MHz, $CDCl_3$) spectrum of compound **2**.

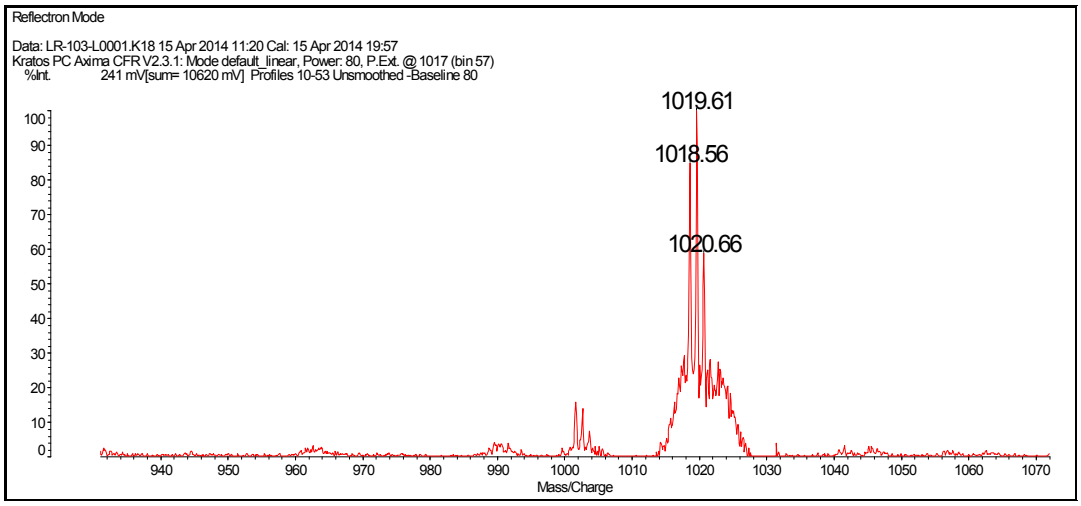

Fig. S6. MALDI/TOF MS spectrum of **2**.

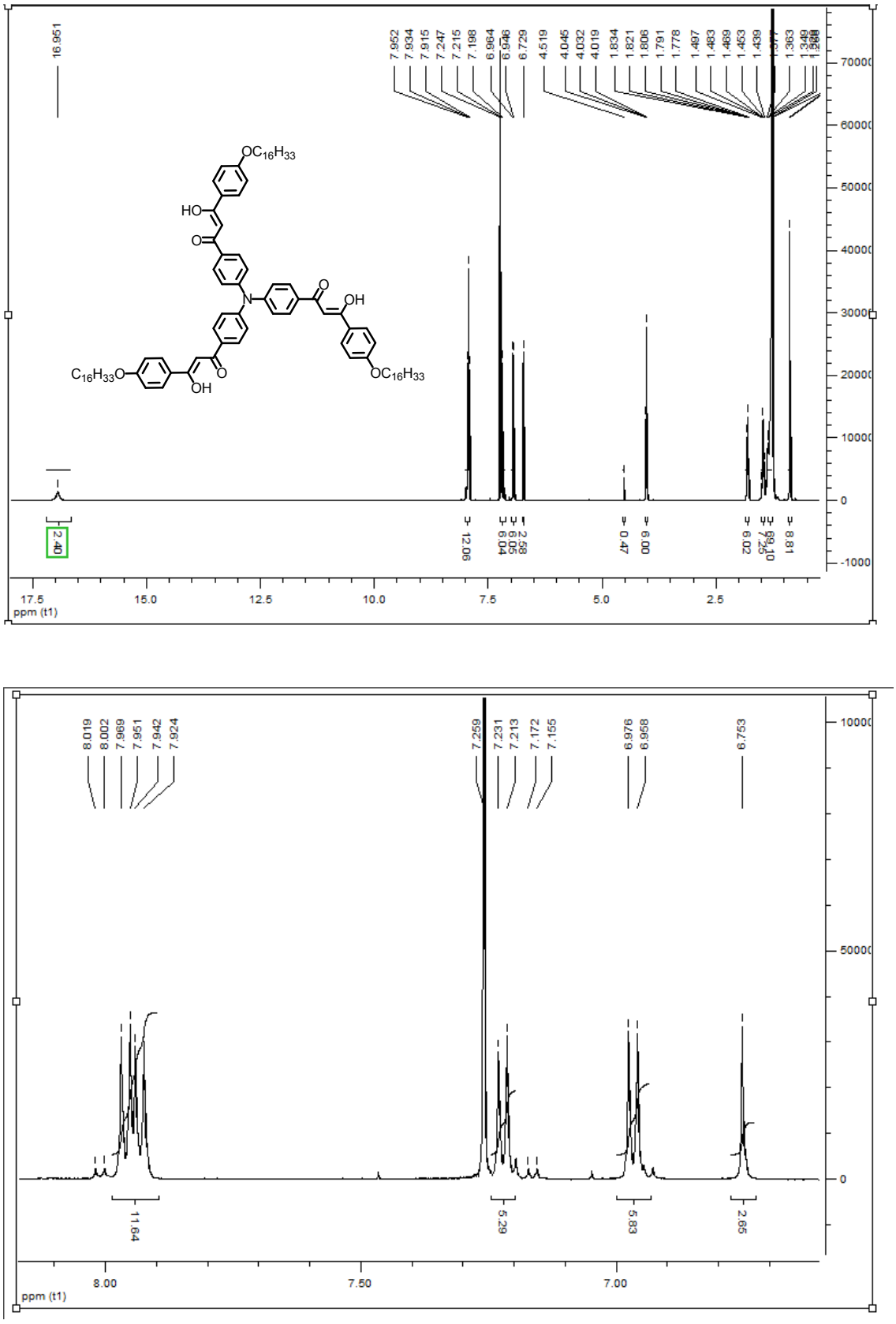

Fig. S7. ^{1}H NMR (400 MHz, $CDCl_3$) spectrum of compound **3**.

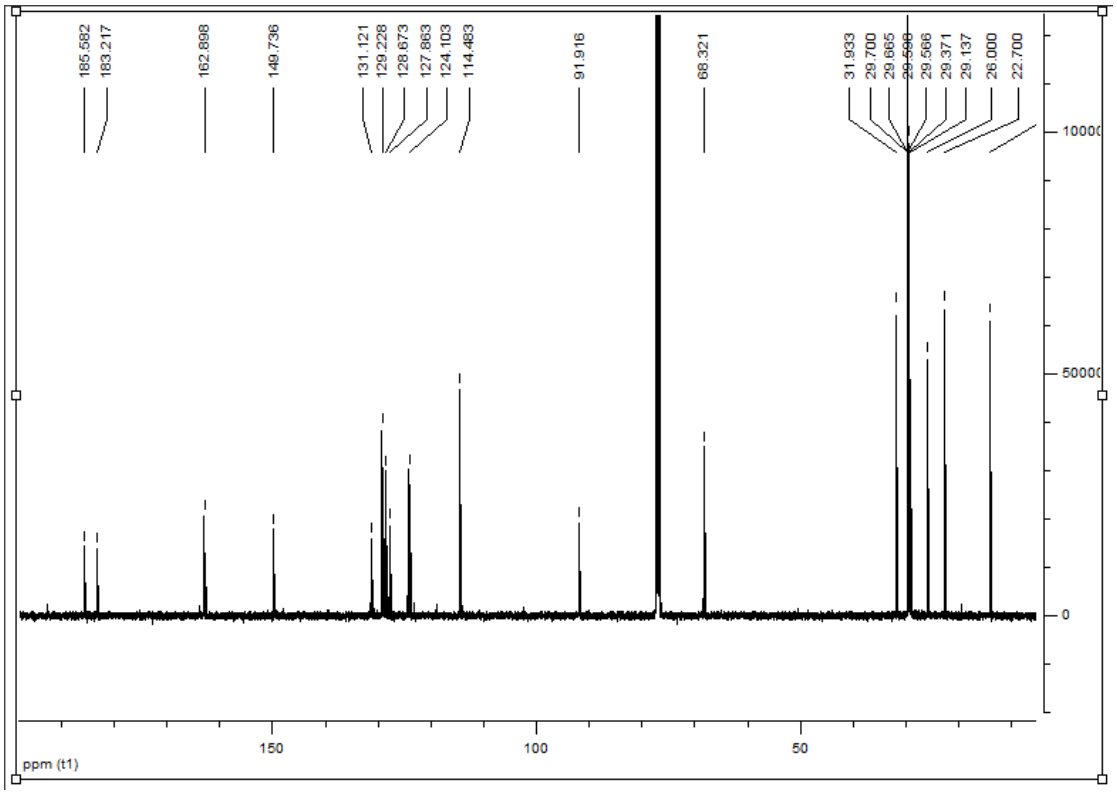

Fig. S8. ^{13}C NMR (125 MHz, $CDCl_3$) spectrum of compound **3**.

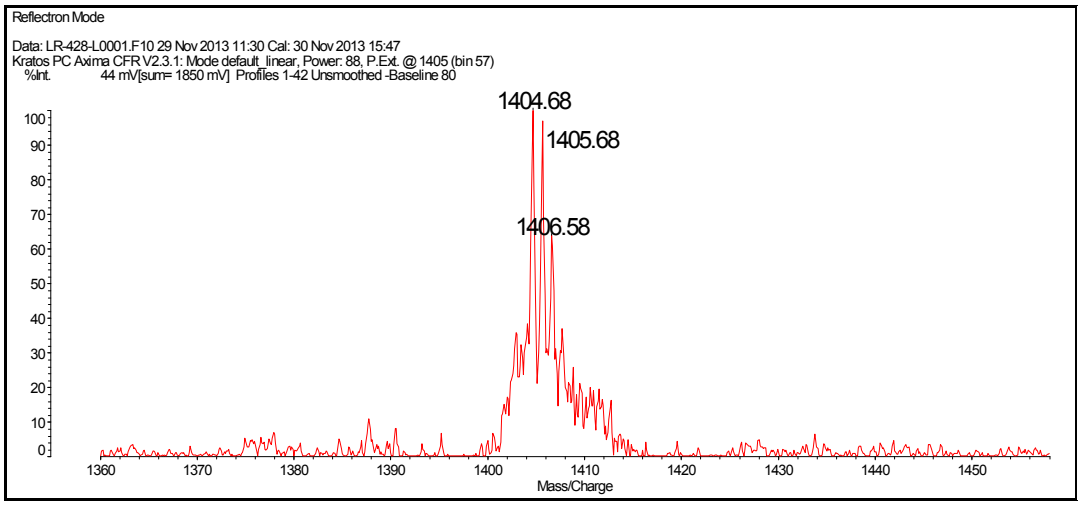

Fig. S9. MALDI/TOF MS spectrum of **3**.

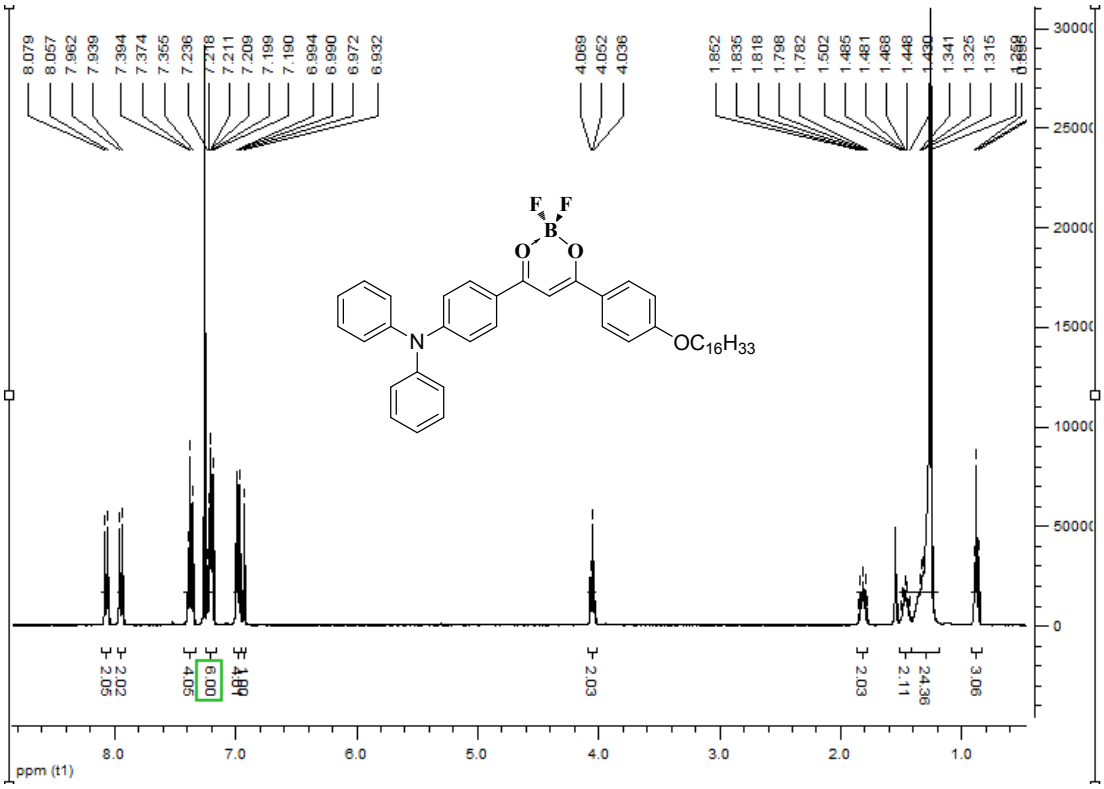

Fig. S10. ^{1}H NMR (400 MHz, $CDCl_3$) spectrum of compound **1B**.

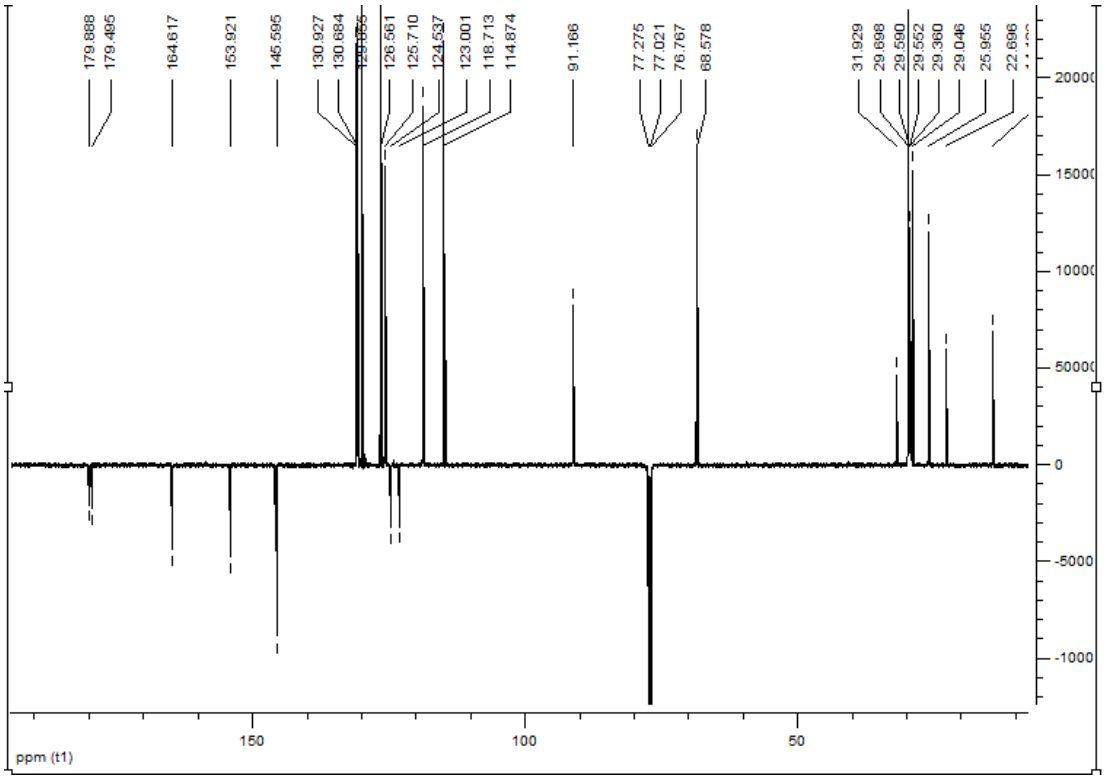

Fig. S11. ^{13}C NMR (125 MHz, $CDCl_3$) spectrum of compound **1B**.

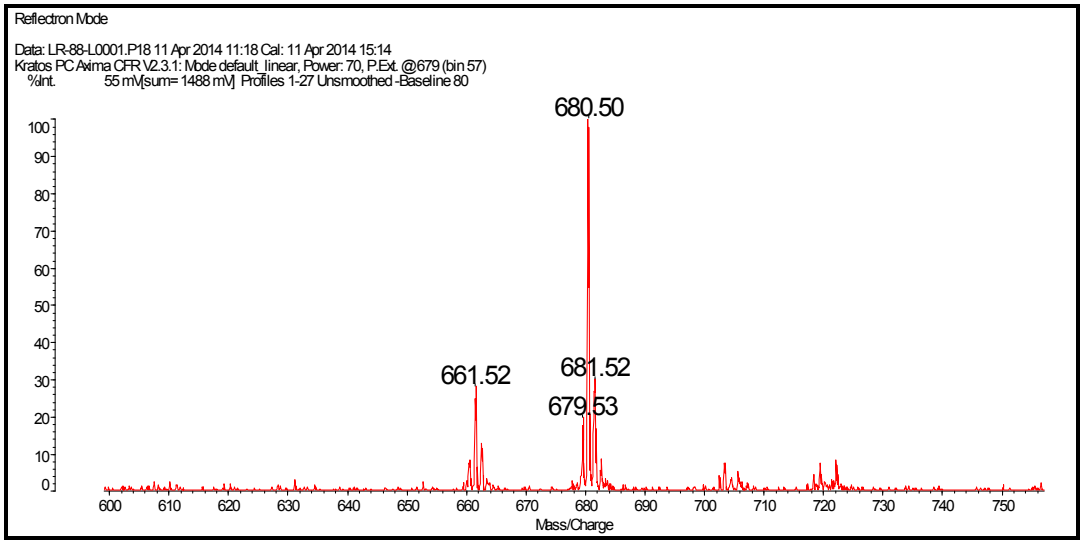

Fig. S12. MALDI/TOF MS spectrum of **1B**.

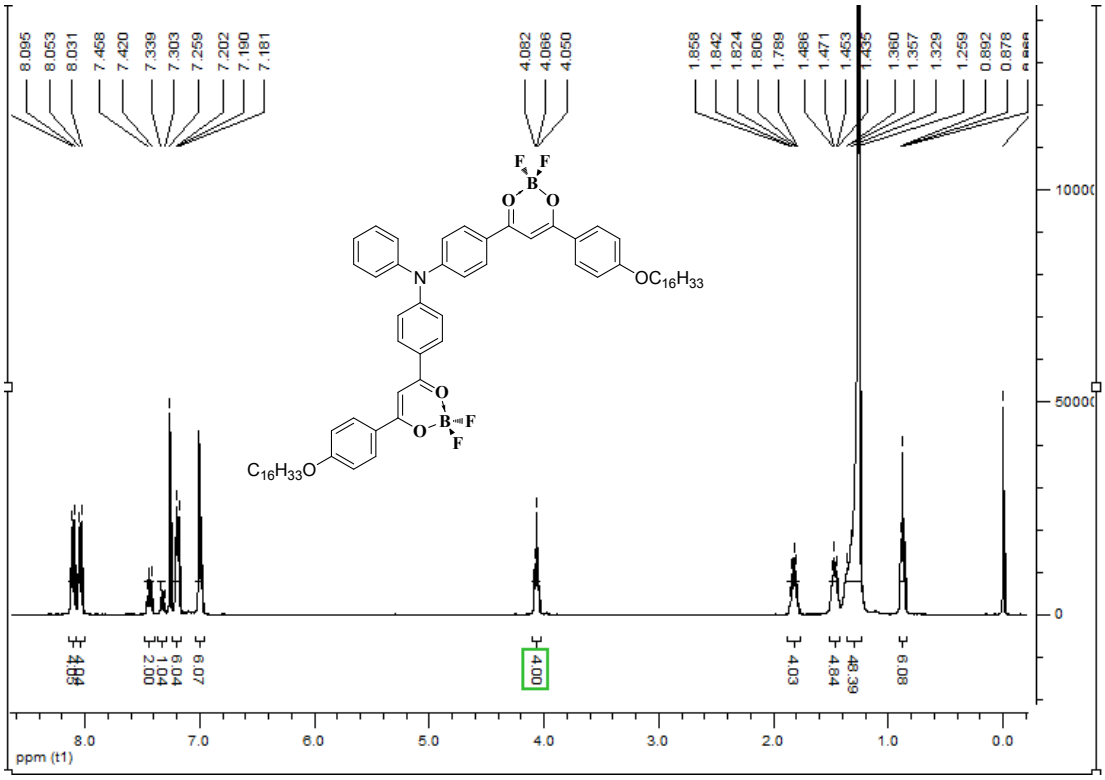

Fig. S13. ^{1}H NMR (400 MHz, $CDCl_3$) spectrum of compound **2B**.

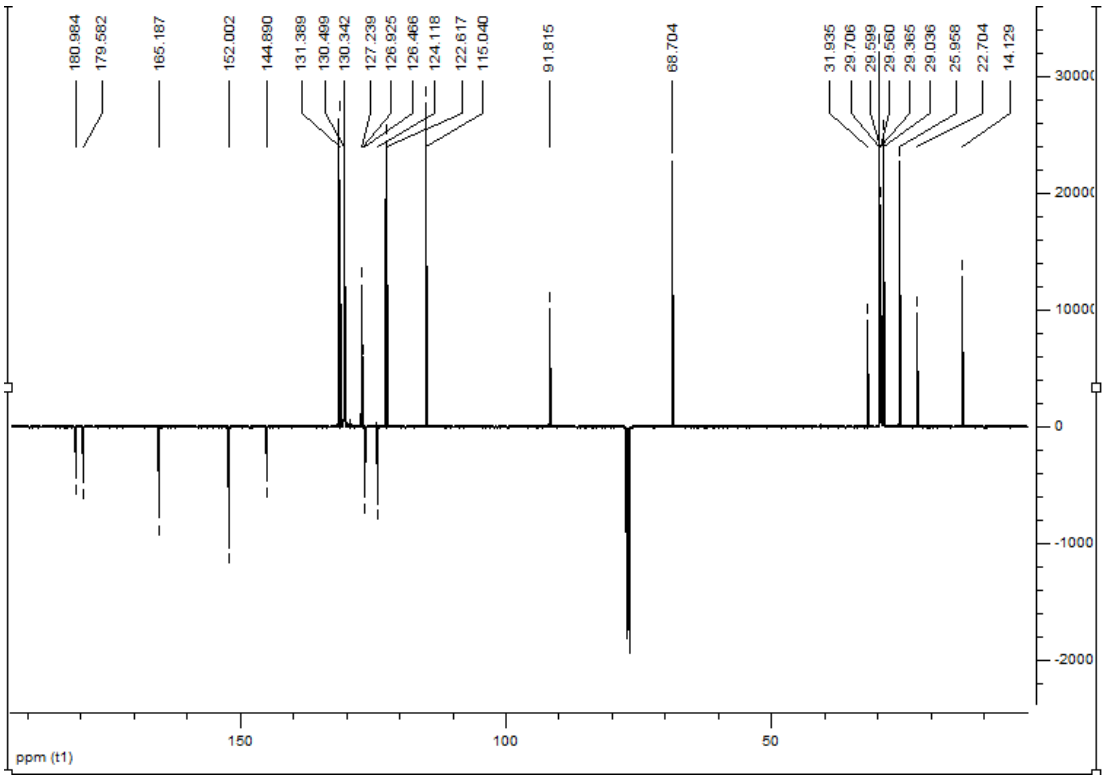

Fig. S14. ^{13}C NMR (125 MHz, $CDCl_3$) spectrum of compound **2B**.

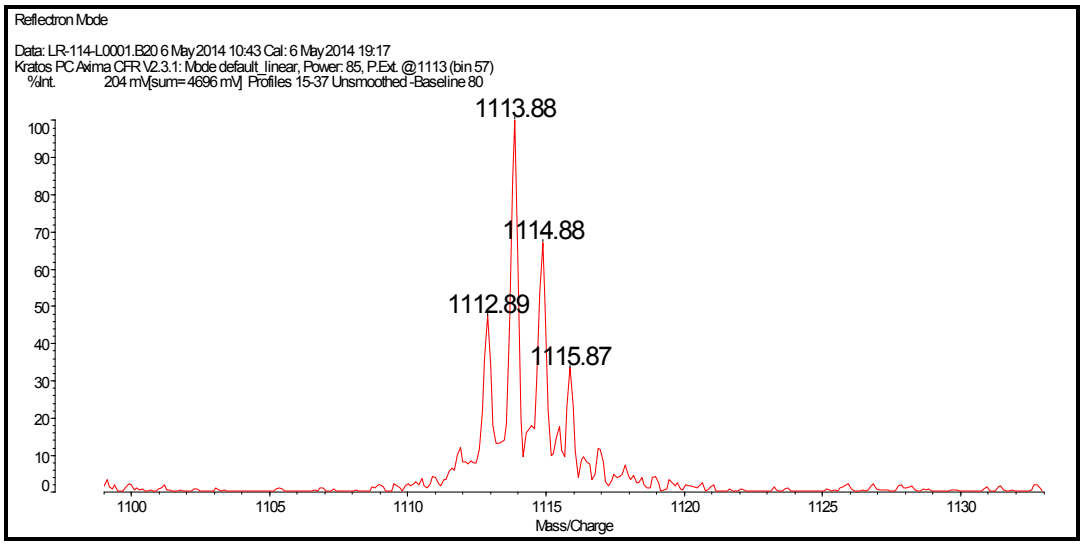

Fig. S15. MALDI/TOF MS spectrum of **2B**.

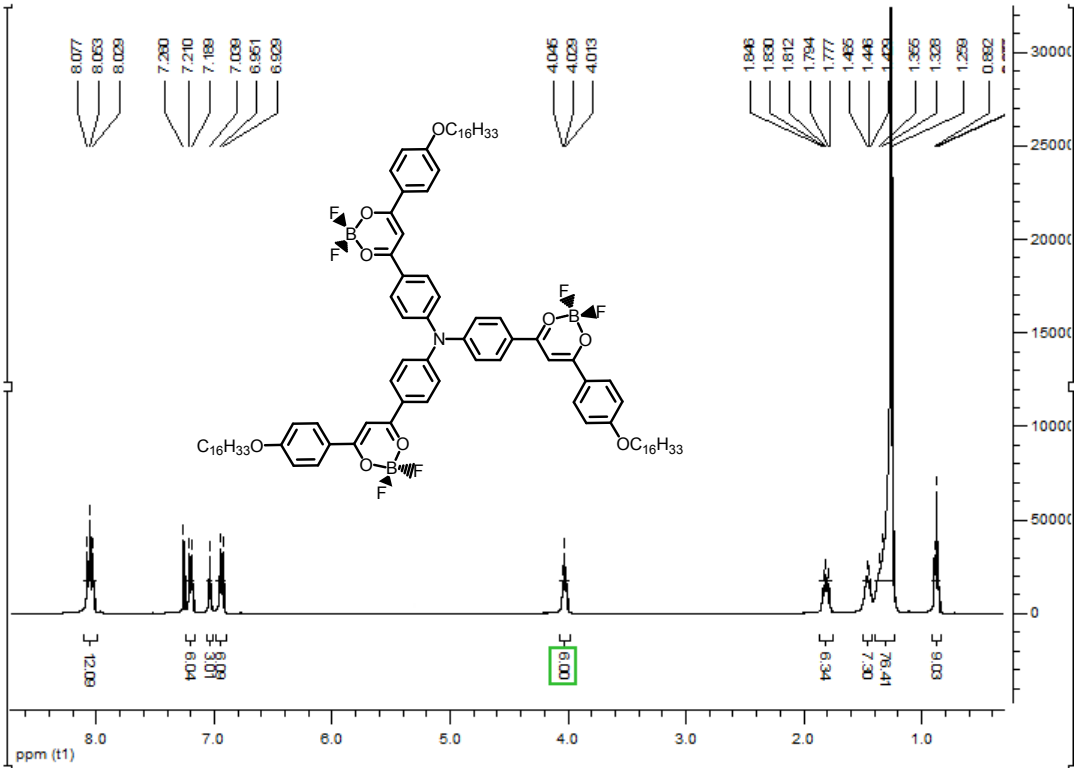

Fig. S16. ^{1}H NMR (400 MHz, $CDCl_3$) spectrum of compound **3B**.

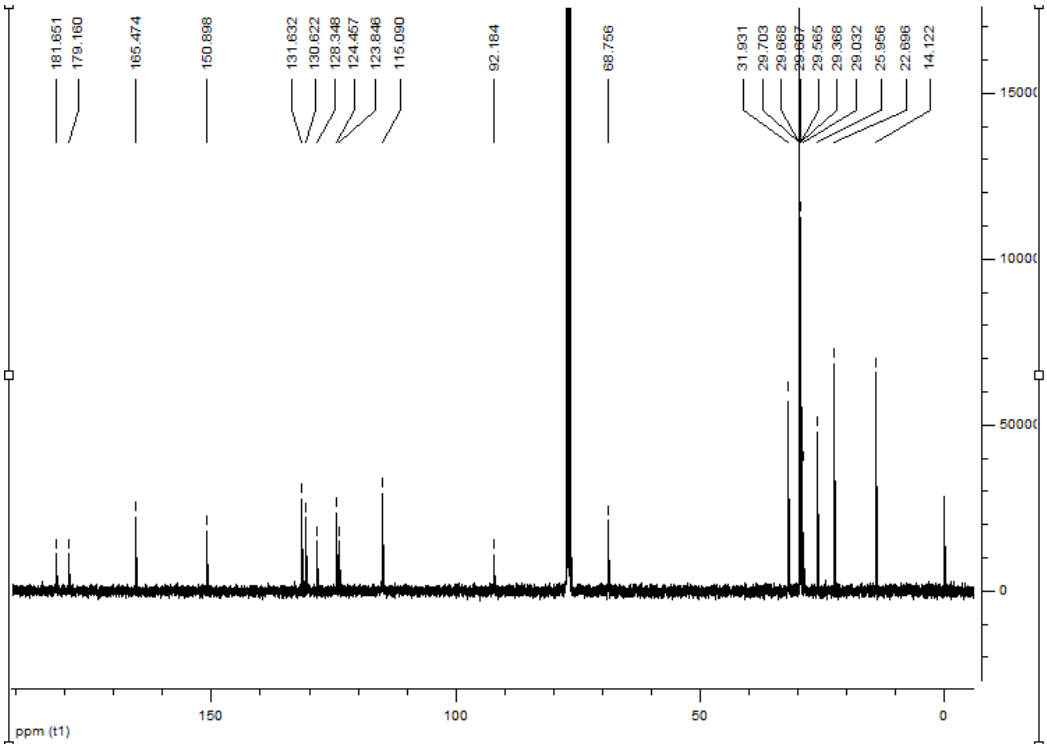

Fig. S17. ^{13}C NMR (125 MHz, $CDCl_3$) spectrum of compound **3B**.

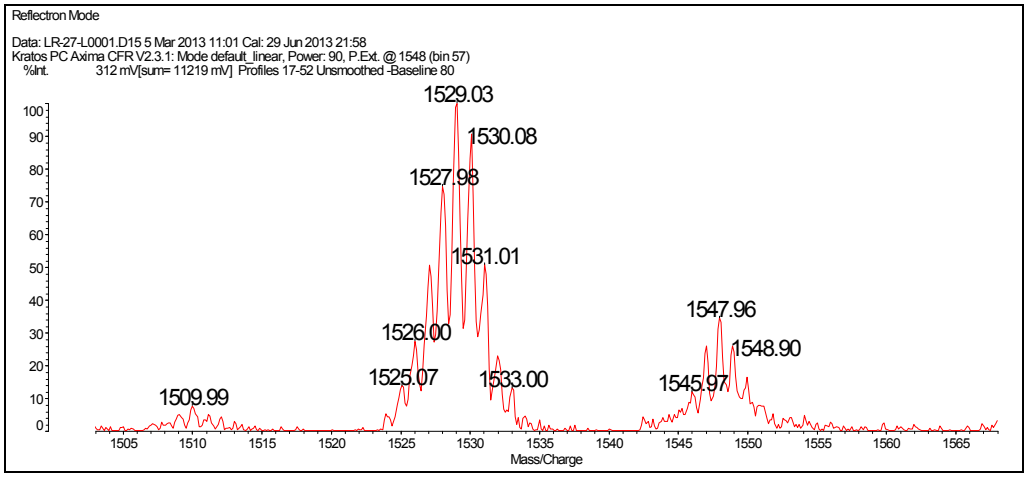

Fig. S18. MALDI/TOF MS spectrum of **3B**.

Table S1. Photophysical data of ligands **1-3** and complexes **1B-3B**.

Compound	in toluene			in solid state	
	λ_{abs}^{max}/ nm (ε_{max} [a])	λ_{em}/ nm	Φ_f [b]	λ_{em} [c]/ nm	Φ_f [d]
1	408 (4.22)	462	0.53	498	0.43
2	427 (6.40)	460	0.57	502	0.11
3	422 (10.28)	454	0.54	517	0.10
1B	467 (6.21)	547	0.60	616	0.25
2B	490 (8.99)	525	0.82	609	0.14
3B	479 (15.62)	510	0.76	604	0.66

[a] M^{-1} cm^{-1}, $\times 10^4$.

[b] Determined by a standard method.[1] For **1-3**, diphenylanthracene (Φ_f = 0.85, λ_{ex} = 390 nm, in benzene) was used as reference.[2] For **1B-3B**, fluorescein (Φ_f = 0.88, λ_{ex} = 460 nm, in 0.1 N NaOH) was used as reference.[3]

[c] The films were obtained by dropping the solutions in dichloromethane (1.0×10^{-4} M) on quartz slide.

[d] Measured using an integrating sphere.

Table S2. Photophysical data of **1-3** in different solvents.

Compound	Solvents	λ_{abs}^{max}/ nm (ε_{max} [a])	λ_{em}/ nm	stokes shift [b]/ nm	fwhm/ nm	Φ_f [c]
1	Toluene	408 (4.22)	457	49	52	0.53
	1,4-Dioxane	408 (4.51)	475	67	81	0.77
	DCM	412 (4.20)	523	111	129	0.57
	DMF	411 (3.62)	539	128	145	0.22
2	Toluene	427 (6.47)	460	33	68	0.57
	1,4-Dioxane	425 (6.40)	468	43	76	0.61
	DCM	430 (6.07)	498	68	106	0.59
	DMF	423 (5.52)	511	78	119	0.37
3	Toluene	422 (10.28)	454	32	53	0.54
	1,4-Dioxane	423 (10.19)	463	40	62	0.52
	DCM	426 (10.04)	488	63	88	0.59
	DMF	429 (7.50)	507	78	103	0.50

[a] M^{-1} cm^{-1}, $\times 10^4$.

[b] Calculated from the difference of λ_{em} and λ_{abs}^{max}.

[c] Fluorescence quantum yield determined by a standard method with diphenylanthracene in benzene (Φ_f = 0.85, λ_{ex} = 390 nm) as reference.

Table S3. Photophysical data of **1B-3B** in different solvents.

Compound	Solvents	λ_{abs}^{max}/ nm (ε_{max} [a])	λ_{em}/ nm	stokes shift [b]/ nm	fwhm/ nm	Φ_f [c]
1B	Toluene	467 (6.21)	547	80	83	0.60
	1,4-Dioxane	466 (6.25)	576	110	112	0.40
	DCM	473 (6.35)	640	167	176	0.02
	DMF	473 (6.70)	-	-	-	-
2B	Toluene	490 (8.99)	525	35	44	0.82
	1,4-Dioxane	491 (9.73)	542	51	78	0.77
	DCM	502 (9.60)	571	69	107	0.41
	DMF	506 (9.23)	616	110	152	0.02
3B	Toluene	479 (15.62)	510	31	42	0.76
	1,4-Dioxane	481 (15.76)	526	45	52	0.71
	DCM	490 (15.28)	550	60	75	0.58
	DMF	498 (15.09)	590	92	96	0.18

[a] M^{-1} cm^{-1}, $\times 10^4$.

[b] Calculated from the difference of λ_{em} and λ_{abs}^{max}.

[c] Fluorescence quantum yield determined by a standard method with Fluorescein in 0.1 N NaOH (Φ_f = 0.88, λ_{ex} = 460 nm) as reference.

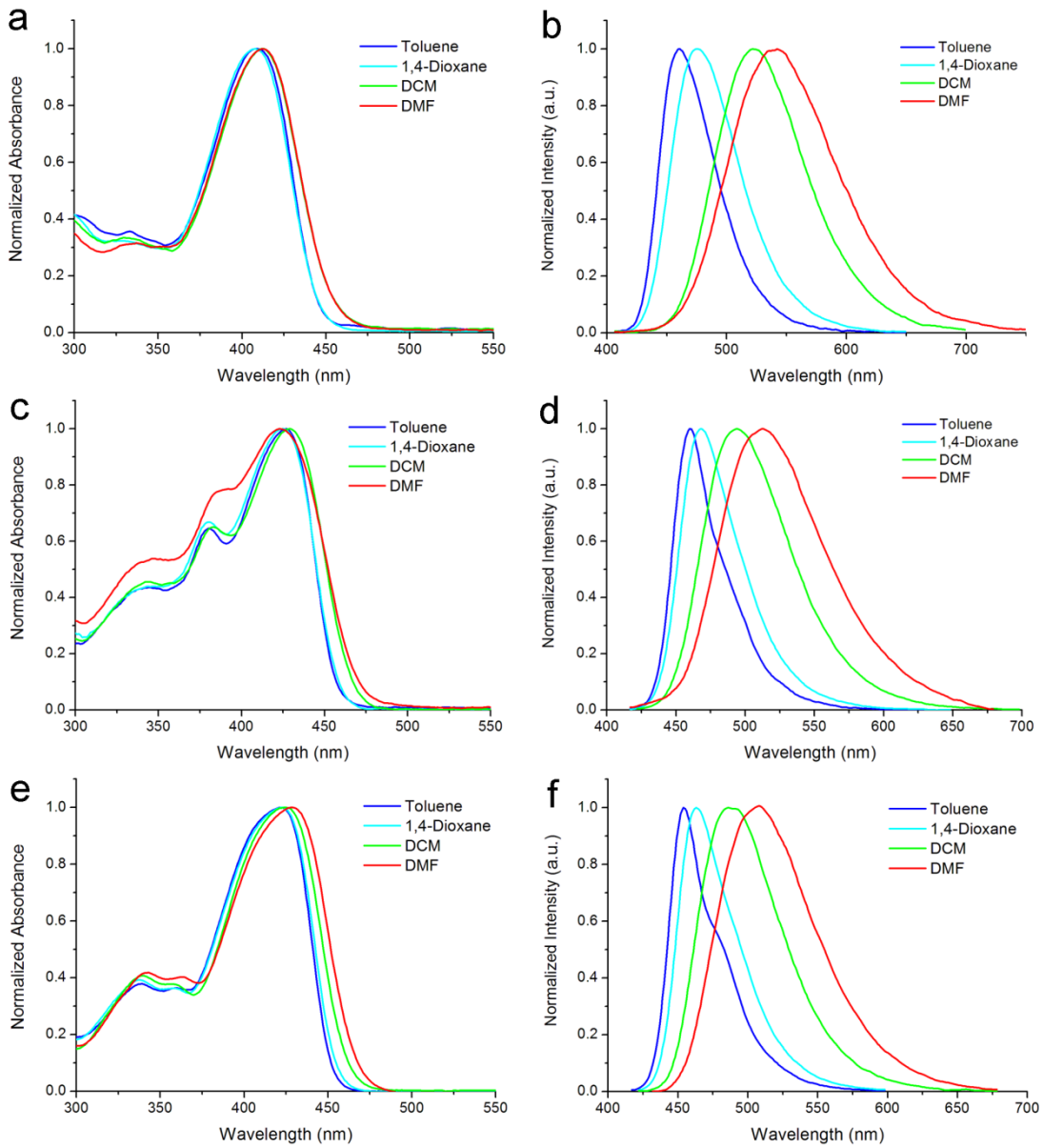

Fig. S19. Normalized UV-vis absorption (a, c and e) and fluorescence emission spectra (b, d and f, λ_{ex} = 400 nm) of **1** (a,b)**, 2** (c,d) and **3** (e,f) in different solvents (2.0×10^{-6} M).

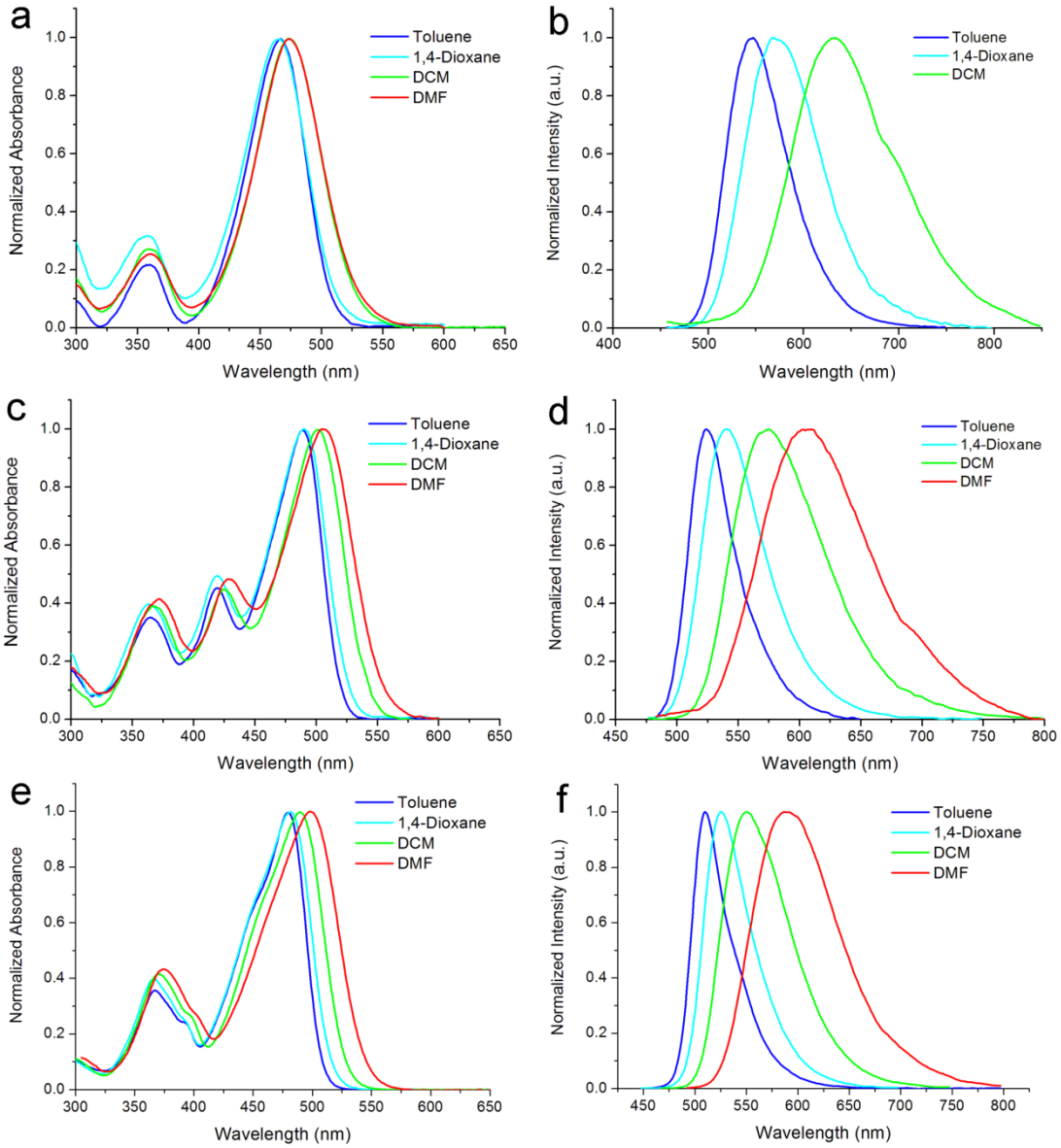

Fig. S20. Normalized UV-vis absorption (a, c and e) and fluorescence emission spectra (b, d and f, λ_{ex} = 450 nm) of **1B** (a,b)**, 2B** (c,d) and **3B** (e,f) in different solvents (2.0×10^{-6} M).

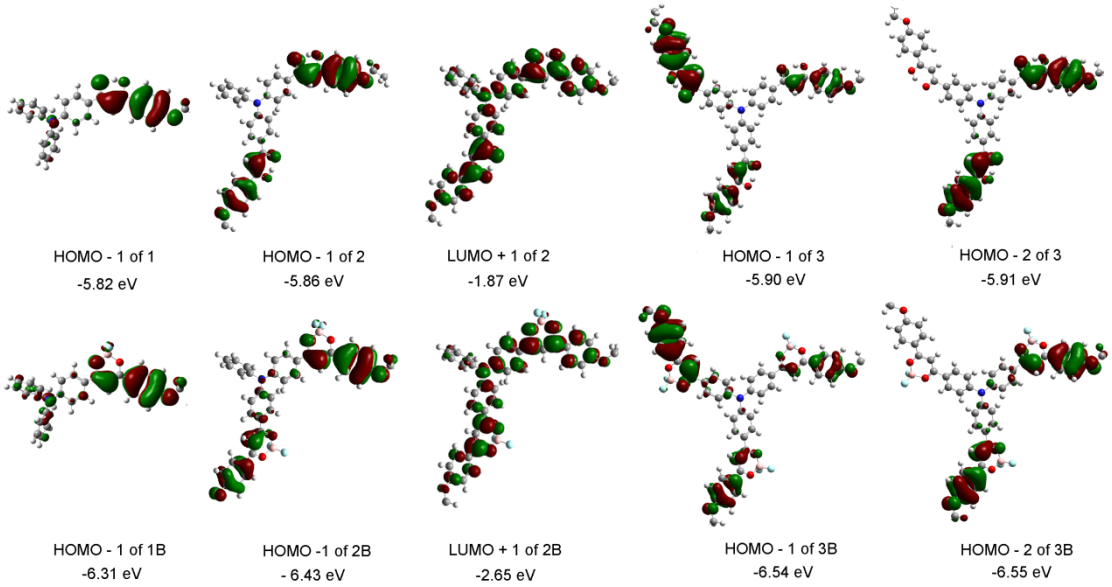

Fig. S21. The energy levels and molecular orbital surfaces in the optimized ground-state structure of β-diketonate **1-3** and complexes **1B-3B**, in which hexadecyl groups were omitted.

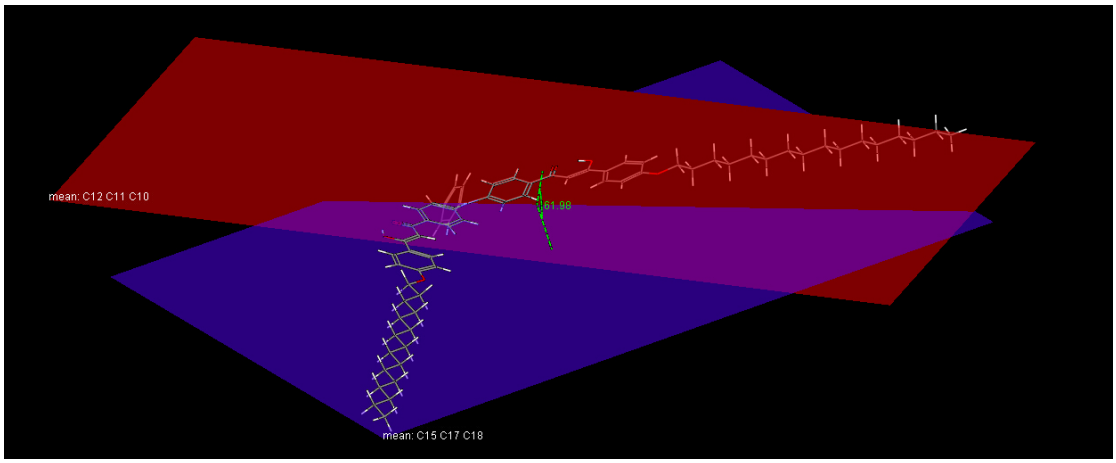

Fig. S22. Illustration of the dihedral angle between two β-diketone units of **2** in optimized structure.

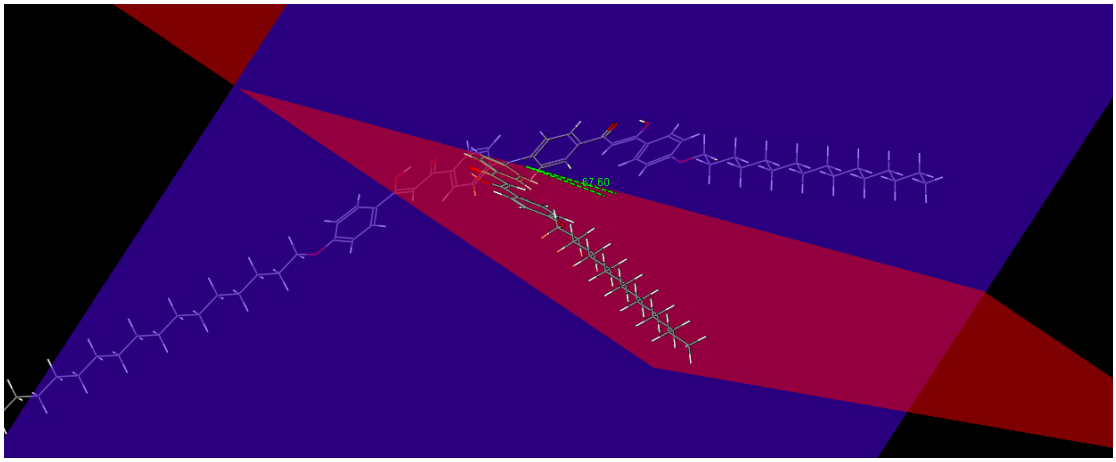

Fig. S23. Illustration of the dihedral angle between two β-diketone units of **3** in optimized structure.

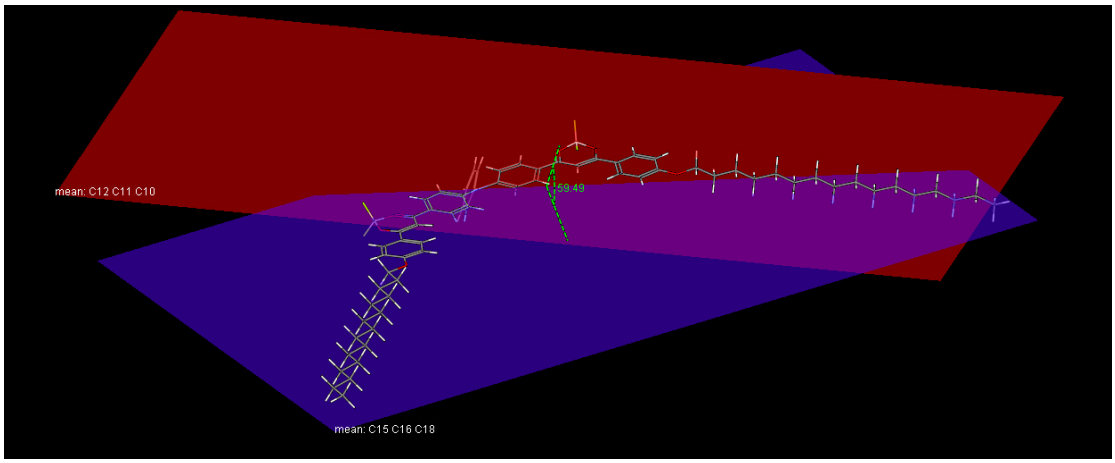

Fig. S24. Illustration of the dihedral angle between two β-diketone units of **2B** in optimized structure.

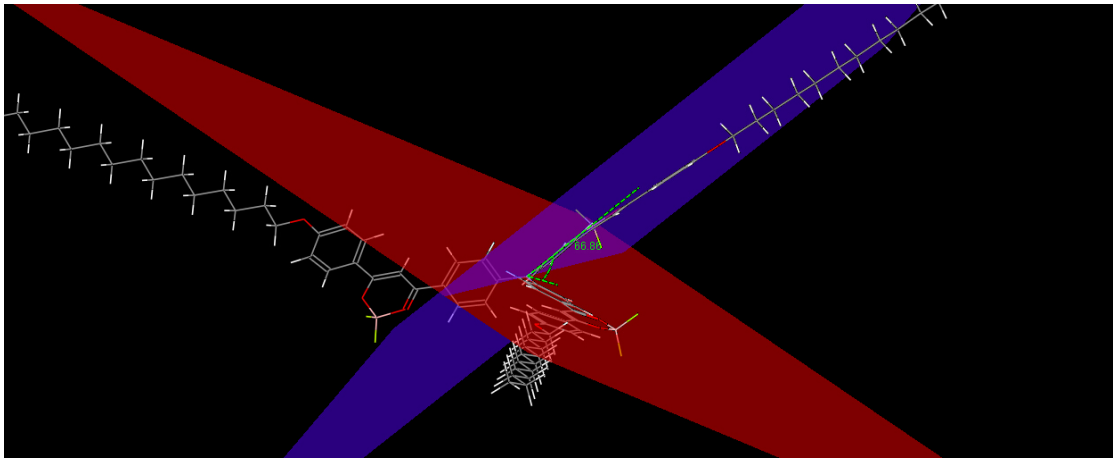

Fig. S25. Illustration of the dihedral angle between two β-diketone units of **3B** in optimized structure.

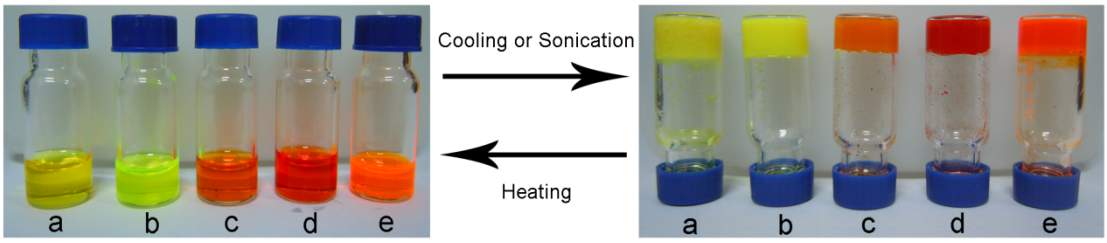

Fig. S26. The photos of the solutions and their corresponding gels of a) **1** in DMSO; b) **3** in DMF; c) **1B** in CH_3COOH/H_2O = 10/1; d) **2B** in DMSO; e) **3B** in heptane.

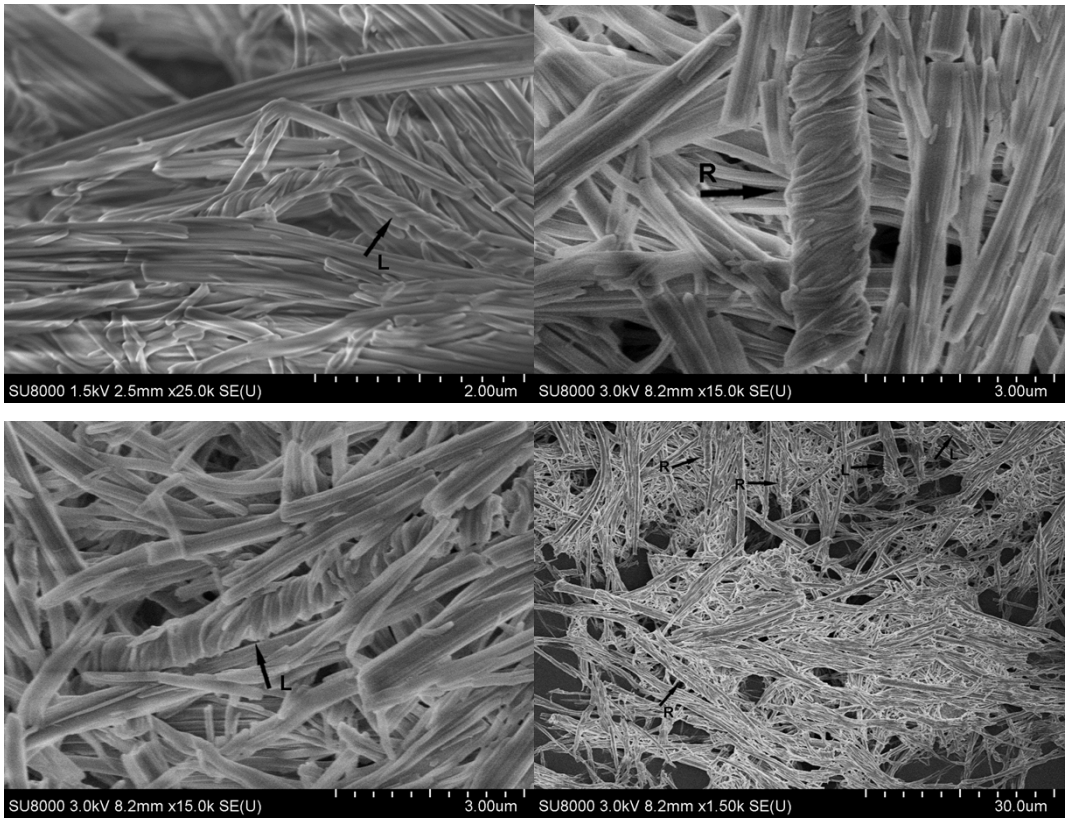

Fig. S27. SEM images of the xerogel **3** obtained from DMF.

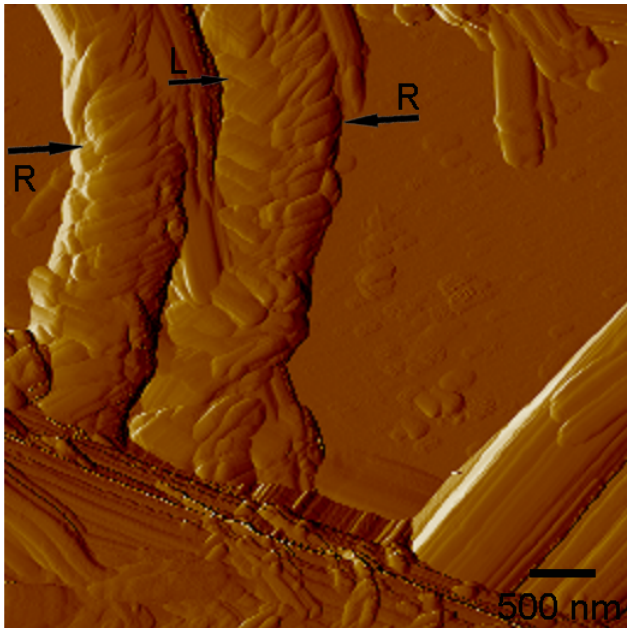

Fig. S28. AFM image of the gel of **3** in DMF.

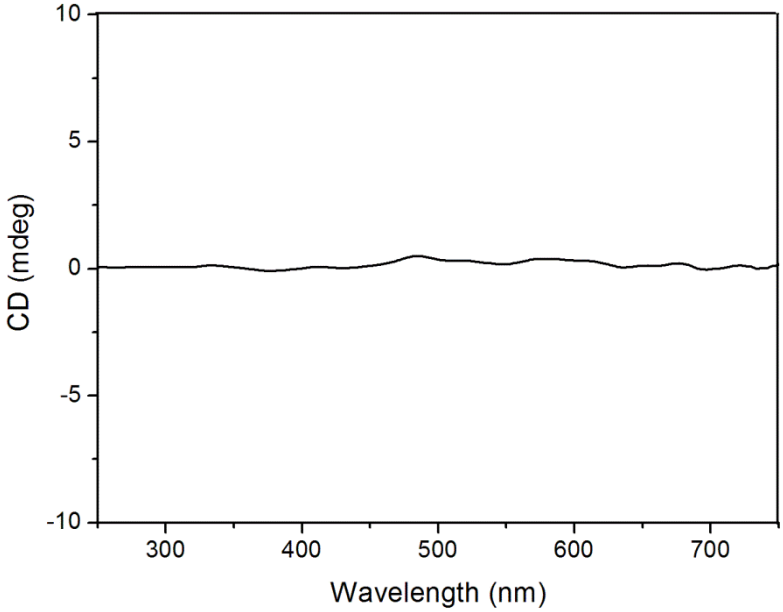

Fig. S29. CD spectra of gel formed from **3** in DMF (8.0 mg/mL).

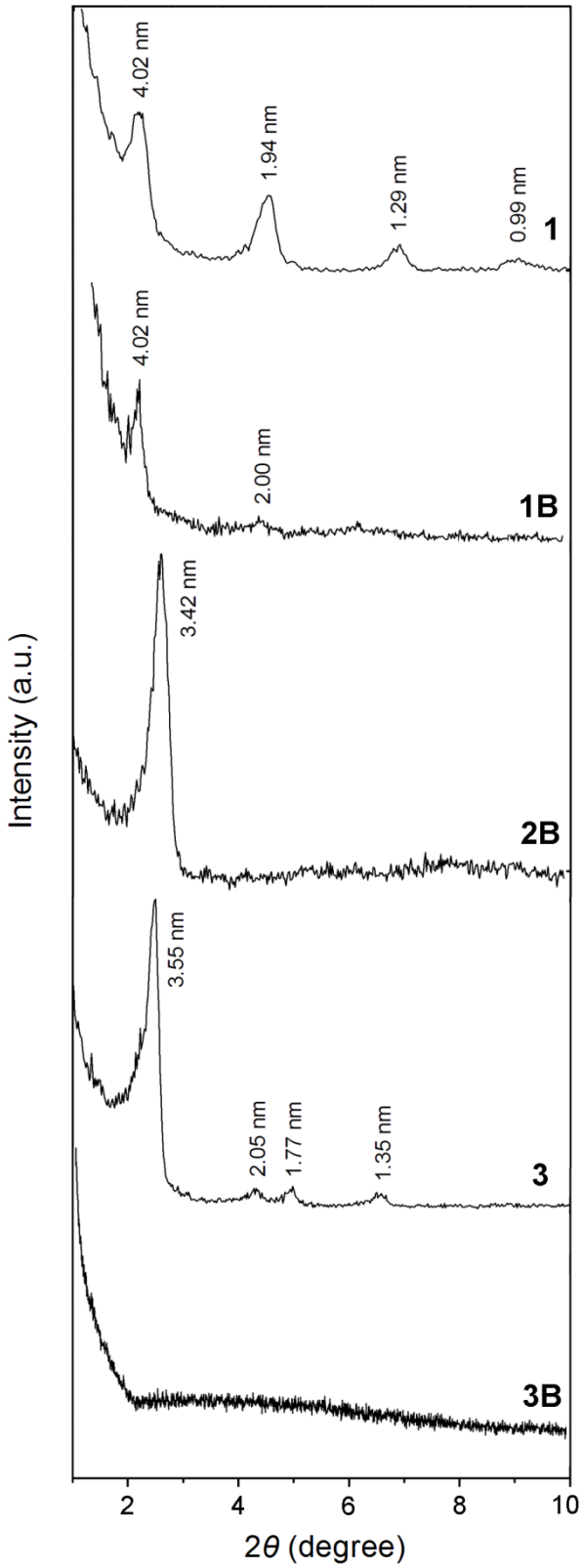

Fig. S30. Small-angle X-ray diffraction patterns of the xerogels of **1** in DMSO, **1B** in CH_3COOH/H_2O = 10/1, **2B** in DMSO, **3** in DMF and **3B** in heptane (from top to bottom).

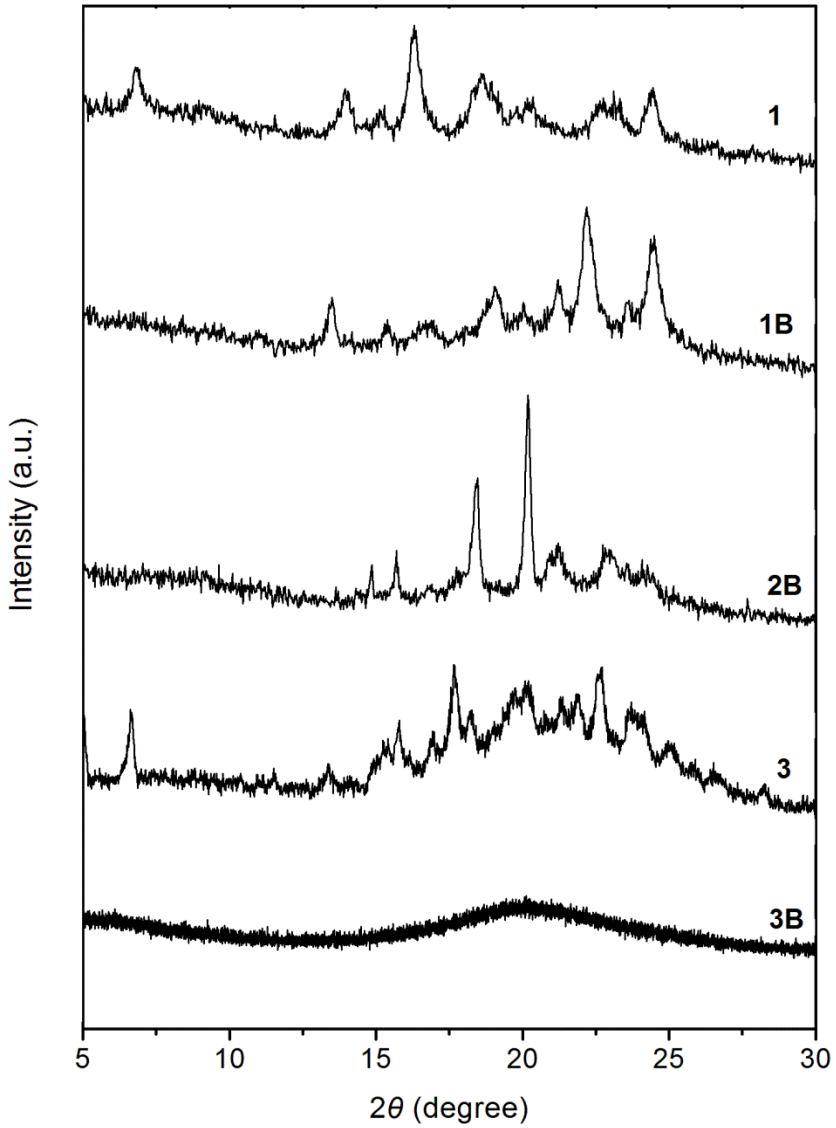

Fig. S31. Wide-angle X-ray diffraction patterns of the xerogels of **1** in DMSO, **1B** in CH3COOH/H_2O = 10/1, **2B** in DMSO, **3** in DMF and **3B** in heptane (from top to bottom).

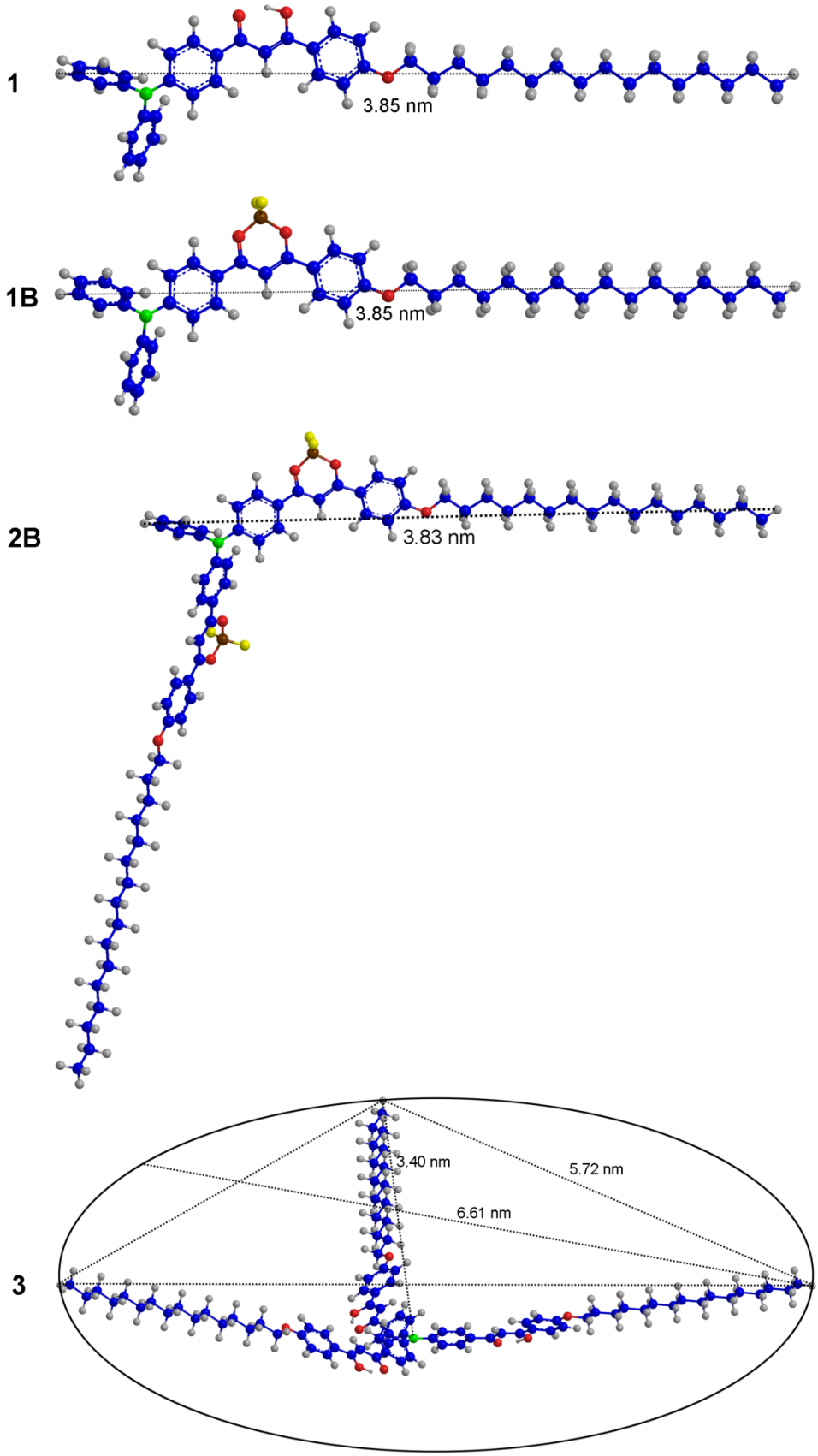

Fig. S32. Optimized geometry structure of **1**, **1B**, **2B** and **3** by DFT calculation.

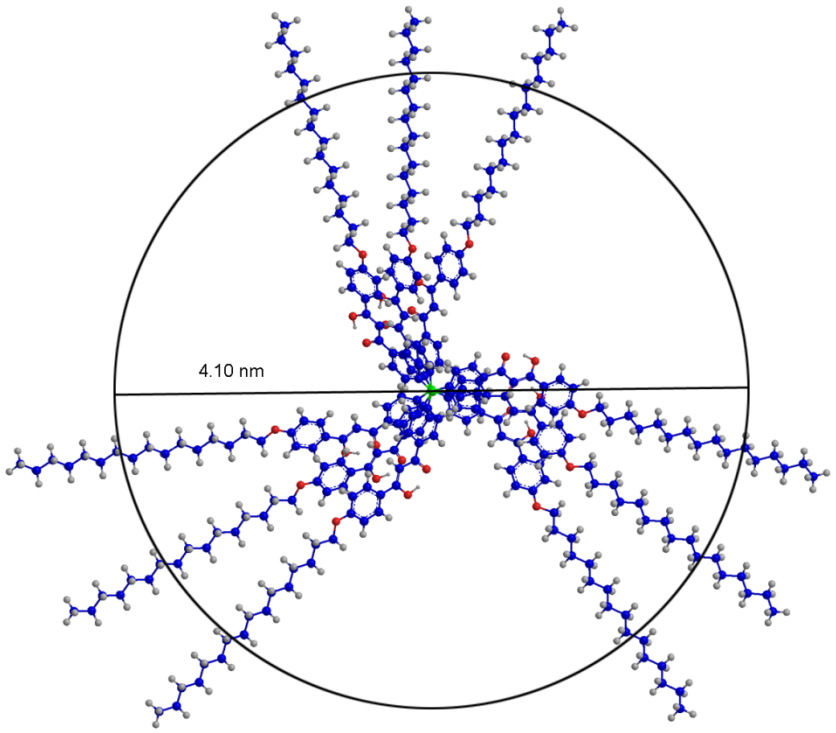

Top view

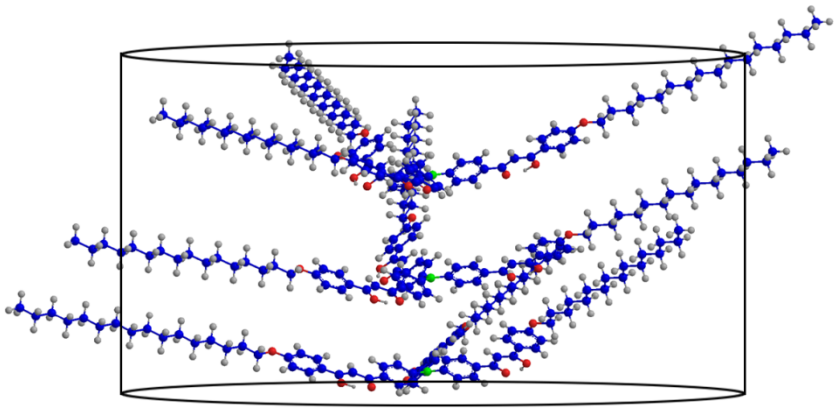

Side view

Fig. S33. Schematic depiction for proposed self-assembled structure from **3** of xerogels.

Refrences

[1] A. D′Aléo, D. Gachet, V. Heresanu, M. Giorgi and F. Fages. *Chem. Eur. J.*, 2012, **18**, 12764 -12772;

[2] H. P. Zhou, X. Zhao, T. H. Huang, R. Lu, H. Z. Zhang, X. H. Qi, P. C. Xue, X. L. Liu and X. F. Zhang. *Org. Biomol. Chem.*, 2011, **9**, 1600-1607;

[3] K. Suzuki, A. Kobayashi, S. Kaneko, K. Takehira, T. Yoshihara, H. Ishida, Y. Shiina, S. Oishi and S. Tobita. *Phys. Chem. Chem. Phys.*, 2009, **11**, 9850-9860.